*Journal of the European Ceramic Society* **15** (1995) 445–453

0955-2219/95/$9.50

0955-2219(95)00004-6

# On the Thermal Degradation of Lox-M Tyranno® Fibres

Constantin Vahlas[a] & Marc Monthioux

Laboratoire Marcel Mathieu, CNRS-UPPA, Centre Hélioparc, 2, avenue Angot, F-64000 Pau, France

(Received 21 April 1994; revised version received 30 September 1994; accepted 12 December 1994)

***Abstract***

*A calculational thermodynamic investigation of the thermal degradation of the Lox-M Tyranno® fibre in inert gas flow at atmospheric pressure has been performed, based on the minimization of the Gibbs energy of the Si–C–O–Ti chemical system. The results are compared to a recent characterization of the material by Transmission Electron Microscopy (TEM) which illustrates its sequential structures and nanotextures as a function of treatment temperature. The degradation mechanisms and the corresponding temperature ranges of this and of the NL-202 Nicalon® fibre in the same conditions are compared and the observed differences are attributed to diffusion-based phenomena.*

## Introduction

The introduction of small amounts of titanium (less than 10 wt%) in silicon oxycarbide ceramic fibres, was first proposed in the early eighties.[1] The aim was to retard crystallization and grain growth at elevated temperatures and hence improve strength retention,[2] and also to improve compatibility for aluminum matrix composites on account of less reactivity but better wettability against molten aluminum.[3] These fibres are produced from organometallic precursors containing Si–O–Ti bonds (polytitanocarbosilane) which are typically obtained using polycarbosilane (PCS) and titanium compounds like tetra-alkoxide,[1,4] tetra-butoxide,[2] or tetra-isopropoxide.[5]

Tyranno® is the family name of a series of non-crystalline Si–Ti–C–O–H fibres fabricated by UBE Industries (Ube, Japan). Since the first publication on this material in 1984,[6] different grades have been presented. Their chemical composition varies between the following values (Ref. 7 and UBE Industries data from Tyranno® fibre, 1986 commercial brochure): Si 45–57, C 25–32, Ti 1·5–4·0, O 12–18, B ≤ 0·15, and N ≤ 0·2 wt%, together with a small amount of hydrogen as a residue of the precursor material. Low oxygen grades of this fibre have recently been commercialized. As for other similar ceramic materials, Tyranno® fibres have valuable mechanical properties up to temperature limits dependent on the operating conditions.

This paper presents a thermodynamic simulation of the behavior of the Lox-M grade of the Tyranno® fibre, under high temperature treatment at atmospheric pressure and inert gas environment. The principle and the different types of calculations as a function of the experimental situation to be simulated are discussed, together with the critical selection of the thermodynamic data for the species considered. The results of calculations are presented by means of yield diagrams, indicating the number of moles obtained at equilibrium for the condensed and the gaseous species as a function of temperature. The theoretical work is associated to a Transmission Electron Microscopy (TEM) investigation which has been presented in part in,[8] with the aim to determine the crystalline structure and nanotexture of the material in the as-received state as well as after thermogravimetric heat treatments at different temperatures, in non-oxidizing environments. This combined approach is expected to allow the stability limit of the fibre, in the investigated conditions, to be determined and to be attributed to corresponding nanotextural changes and chemical reaction mechanisms. The results are compared to the thermal behavior of the NL-202 Nicalon® fibre (Nippon Carbon), which is aimed at similar applications but contains no titanium.

## Thermodynamics

The calculations are based on the minimization of the total Gibbs energy ($G$) of the chemical system generated from combinations of the elements

[a]Permanent address: Laboratoire de Matériaux, URA 445, ENS Chimie, 118 route de Narbonne, F-31077 Toulouse, France.

Si–C–O–Ti–Ar and they were performed by using the GEMINI2 software.[b] Twenty four condensed stoichiometric compounds and three solution phases (liquid and bcc Ti–Si and fcc Ti–C) were involved in the calculations together with twenty gaseous species.

The gas phase was assumed to be ideal. The equation adopted for the free energy of formation, as a function of temperature, $T$, for each stoichiometric species is:

$$\Delta G^{\circ}(T) = a_1 + a_2T + a_3T\ln T + a_4T^2 + a_5T^3 + a_6T^{-1} + a_7T^4 + a_8T^5 + a_9T^7 + a_{10}T^{-9} + a_{11}\ln T + a_{12}T^{-2} + a_{13}T^{-3} \quad (1)$$

Data were mainly drawn from the Scientific Group Thermodata Europe (SGTE) data bank[9] and from Barin's compilation.[10] Data on $Si_xC_y$ species were drawn from Gurvich *et al.*[11]

The excess free energy of the solid solutions, $G^{ex}$, was described by a generalized multi-sublattice model as developed by Sundman and Agren,[12] including in particular the classical substitution and the two-sublattice models, applied to the two Ti–Si phases and to the Ti–C phase respectively. For the one sublattice (substitution) model, $G^{ex}$ is written:

$$G^{ex} = x_{Ti}x_{Si}L_{Ti,Si}(x,T) \quad (2)$$

where $x_i$ is the atomic fraction of the component i and $L_{Ti,Si}(x,T)$ is the binary interaction term:

$$L_{Ti,Si}(x,T) = \sum_{\nu}(x_{Ti} - x_{Si})^{\nu}L^{(\nu)}_{Ti,Si}(T) \quad (3)$$

$L^{(\nu)}_{Ti,Si}(T)$ being a binary interaction parameter of order v between Ti and Si, depending on temperature according to the relation (1). Data for these solution phases comes from Vahlas *et al.*[13] In the two sublattice model, applied to the Ti–C phase, the first and the second sublattices are considered to be filled by the carbon atoms or vacancies and by the titanium atoms respectively. In that case, $G^{ex}$ is written:

$$G^{ex} = y_Cy_{vac}L_{C,vac:Ti}(y,T) \quad (4)$$

where $y_c$, $y_{vac}$ are the atomic fractions of C and of vacancies on their sublattice ($y_c + y_{vac} = 1$) and $L_{C,vac:Ti}$ is the binary interaction parameter between carbon and vacancies within the corresponding sublattice:

$$L_{C,vac:Ti}(y,T) = \sum_{\nu=0}^{\nu}(y_C - y_{vac})^{\nu}L^{(\nu)}_{C,vac:Ti}(T) \quad (5)$$

Although Vincent *et al.*,[14] propose an eight term function for $L_{C,vac:Ti}$, (with $\nu = 4$ and $L^{(\nu)}_{C,vac:Ti} = a +$

[b]Gibbs Energy MINIminimizer (GEMINI2), available from THERMODATA, BP66, F-38402 Saint Martin d'Hères, France.

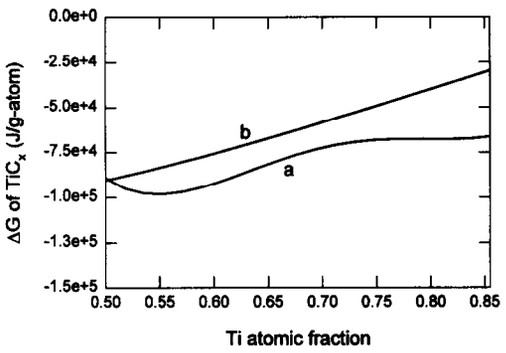


**Fig. 1.** Free energy of the Ti–C solid solution as a function of Ti atomic fraction for T = 800 K (527°C). (a) Vincent *et al.*[14] model; (b) present model.

$bT$), in these calculations we used a simpler and more realistic description where $L_{C,vac:\ Ti} = -6000$ J/g-atom. This eliminates demixing artifacts as shown for example in Fig. 1, where the free energy of $TiC_x$ is drawn at 800 K (527°C) as a function of the Ti atomic fraction, using the models adopted in[14] (a), and in this work (b). However, a complete re-calculation of the Ti–C system with regard to available metallurgical and thermodynamic experimental data, as attempted in,[14] remains to be done.

There is no thermodynamic data available for the amorphous $SiC_xO_y$ solid solution although there is strong evidence in the literature for the existence of this phase.[15–20] Consequently, although this phase is possibly present in the as-received material, by analogy with the NL-202 Nicalon® fibre as was shown among others in Ref. 20 it was replaced in calculations by an equivalent mixture of SiC+$SiO_2$+C. This assumption, the validity of which we have discussed in recent work,[21] does not allow the specific evolution of the fibre during the transition period of degradation to be simulated. However, it is expected to have little influence on the calculated degradation temperature and on the fibre and gas phase composition above it. Indeed, as is evidenced by the elemental analysis and the TEM investigation, there is no $SiC_xO_y$ solid solution left at the end of the degradation process of the NL-202 Nicalon® fibre. By analogy with the above, no $SiTi_xC_yO_z$ solid solution was considered in the calculations.

The models for the ternary $Ti_3SiC_2$ and $Ti_5Si_3C_x$ compounds come from Racault *et al.*[22] Because of lack of data on the $Ti_5Si_3C_x$ solution phase, the authors considered it as a $Ti_{0.6}Si_{0.34}C_{0.05}$ stoichiometric compound.

Each phase of each chemical element considered (Si, C, O, Ti) was incorporated in the calculations as a $G$–$H_{ser}$ function of temperature, equivalent to the expression (2). $G$–$H_{ser}$ is the Gibbs energy relative to the enthalpy of the 'Standard Element Reference', i.e. the reference phase of the element at

**Table 1.** Species considered in the thermodynamic calculations and the origin of their thermodynamic description.

| *No.* | *Species* | *Ref.* | *No.* | *Species* | *Ref.* | *No.* | *Species* | *Ref.* | *No.* | *Species* | *Ref.* |
|---|---|---|---|---|---|---|---|---|---|---|---|
| 1 | C-diamond | 23 | 14 | $TiO_2$-(S)A | 9 | 26 | Ti–Si-bcc | 13 | 38 | CO-gas | 10 |
| 2 | C-graphite | 23 | 15 | $Ti_2O_3$-solid | 9 | 27 | Ti–Si-liquid | 13 | 39 | $CO_2$-gas | 10 |
| 3 | Si-diamond | 23 | 16 | $Ti_3O_5$-solid | 9 | | | | 40 | SiC-gas | 11 |
| 4 | Ti-hcp | 11 | 17 | $Ti_4O_7$-solid | 9 | 28 | C-gas | 10 | 41 | $SiC_2$-gas | 11 |
| 5 | SiC-hex., liquid | 11 | 18 | TiSi-solid | 13 | 29 | $C_2$-gas | 10 | 42 | $Si_2C$-gas | 11 |
| 6 | SiC-cubic | 11 | 19 | $TiSi_2$-solid | 13 | 30 | $C_3$-gas | 10 | 43 | SiO-gas | 10 |
| 7 | $SiO_2$-Lquartz | 9 | 20 | $Ti_3Si$-solid | 13 | 31 | O-gas | 10 | 44 | $SiO_2$-gas | 11 |
| 8 | $SiO_2$-Hquartz | 9 | 21 | $Ti_5Si_3$-solid | 13 | 32 | $O_2$-gas | 23 | 45 | TiO-gas | 9 |
| 9 | $SiO_2$-tridymite | 9 | 22 | $Ti_5Si_4$-solid | 13 | 33 | $O_3$-gas | 10 | 46 | $TiO_2$-gas | 9 |
| 10 | $SiO_2$-cristobalite | 9 | 23 | $Ti_3SiC_2$-solid | 22 | 34 | Si-gas | 10 | 47 | Ar-gas | 23 |
| 11 | $SiO_2$-liquid | 9 | 24 | $Ti_5Si_3C_x$-solid | 22 | 35 | $Si_2$-gas | 10 | | | |
| 12 | TiO-solid | 9 | | | | 36 | $Si_3$-gas | 10 | | | |
| 13 | $TiO_2$-(C)R | 9 | 25 | Ti-$C_x$-fcc | 14 | 37 | Ti-gas | 9 | | | |

298 K (20°C). The data adopted for this function come from Dinsdale's compilation.[23]

By analogy with the behavior, in the same conditions, of the NL-202 Nicalon® fibre (as experimentally illustrated in Ref. 20 and simulated in Ref. 21), the de-hydrogenation process is expected to occur in relatively early stages of the thermal treatment yielding molecular hydrogen as the main gaseous by-product. Hence, and since titanium hydrides are not very stable compared to other compounds involved in the calculations, hydrogen and hydrogen-containing species were not considered in this study. The species involved in the calculations and the source of the thermodynamic description adopted are listed in Table 1.

Various quantities of inert gas in contact with the fibre were considered in order to differentiate the chemical environments at the skin and in the core of it. This approach helps to illustrate, in the calculations, the available volume around the fibre and within the pores which may exist within the fibre as was indicated in Ref. 21. Hence, calculations were made with 1 g-atom (skin) and $10^{-4}$ g-atom of Ar (core) in contact with 1 g-atom of the fibre the initial elemental composition of which was experimentally determined as: Si 52·85 (33·23), C 31·64 (46·42), O 13·07 (14·37), Ti 1·85 (0·68) and H <0·30 (<5·28) wt (at)%.

In Fig. 2 the calculated results are presented for the skin environment (1 g-atom Ar/g atom) as a function of treatment temperature. The evolution of the condensed products is illustrated in Fig. 2(a). In these calculations the fibre is represented by a mixture of SiC, C and $SiO_2$ which remains stable up to 1500 K (1227°C). Above this temperature there is a slight decrease of the oxygen and of the free carbon content of the material. At 1600 K (1327°C) the free carbon vanishes while SiC increases significantly. At this temperature, the oxygen content reaches a plateau an order of magnitude below its initial concentration and at 1750 K (1477°C) it also vanishes. The above behavior is related to the evolution in the same operating conditions of the gaseous by-products of the heat treatment, presented in Fig. 2(b). From this figure it appears that silicon and especially carbon monoxides, SiO and CO, are the main gaseous species. Their quantities continuously increase with temperature before reaching a plateau at 1600 K (1327°C) for CO and at 1750 K (1477°C) for SiO, corresponding to the exhaustion of the free carbon and of the oxygen reserves of the fibre respectively. At and beyond 1750 K (1477°C) the quantity of CO is ten times higher than that of SiO. Other species, especially $CO_2$ and Si are present at high temperatures but in very low quantities. They also qualitatively follow the evolution of the free carbon and of the oxygen within the fibre. Beyond 1800 K (1527°C) their increase is delayed or stopped due to the appearance of small quantities of gaseous $Si_xC_y$ species.

From Fig. 2(a) it appears that titanium is found in the fibre exclusively in its carbide form. An expansion on the $y$ axis of the above diagram is presented in Fig. 3, aiming to evidence any minor evolution of $TiC_x$ with temperature. The composition of the $TiC_x$ phase in terms of carbon content for one g-atom of titanium is also presented in this figure. The quantity of $TiC_x$ remains unchanged up to 1650 K (1377°C). Beyond this temperature $TiC_x$ definitively decreases, but not in significant amounts: At 2000 K the number of moles of $TiC_x$, is $7{\cdot}1997 \times 10^{-3}$ to be compared to $7{\cdot}2 \times 10^{-3}$ in the as-received material. The carbon content of the $TiC_x$ phase follows an equivalent evolution: while up to approximately 1600 K (1327°C) titanium carbide remains stoichiometric, beyond this temperature it continuously loses carbon but again in very small amounts: At 2000 K (1727°C) $TiC_x$ is $10^{-4}$ g-atom understoichiometric in carbon. No gaseous Ti-containing compounds are shown in Fig. 2(b). As a matter of fact TiO and Ti

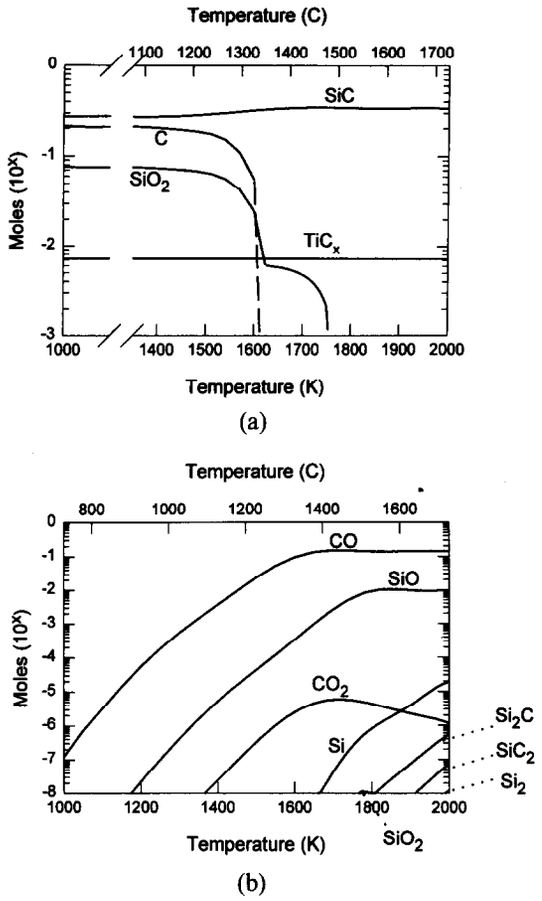


**Fig. 2.** Thermal evolution of one g-atom of Lox-M. Condensed (a) and gaseous (b) species in contact with one g-atom Ar as a function of treatment temperature.

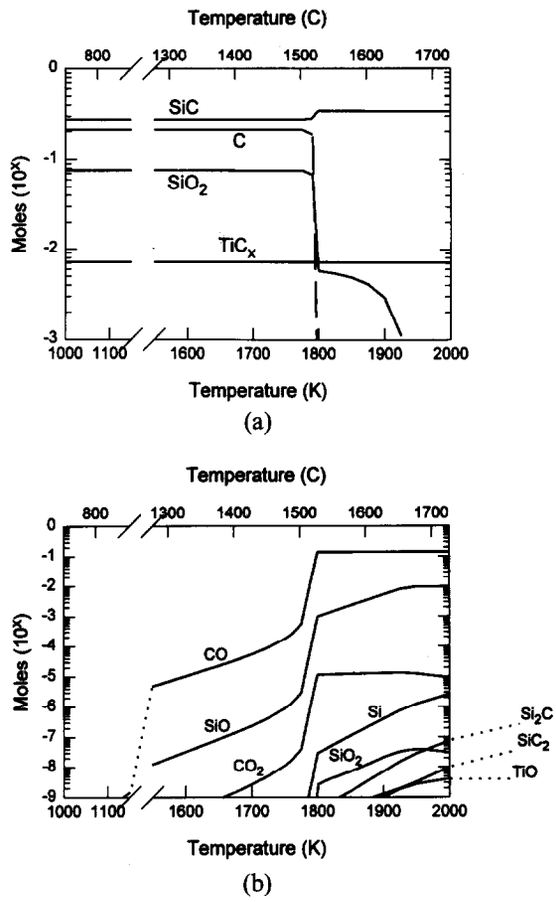


**Fig. 4.** Thermal evolution of one g-atom of Lox-M. Condensed (a) and gaseous (b) species in contact with $10^{-4}$ g-atom Ar as a function of treatment temperature.

appear above 1900 K (1627°C) in extremely low quantities ($<2 \times 10^{-9}$ g-atom) illustrating the stability of carbon and silicon oxides towards titanium compounds.

Figure 4 presents the evolution with temperature of the fibre in contact with $10^{-4}$ g-atom Ar (core), for the condensed species (Fig. 4(a)), and for the gaseous (Fig. 4(b)) species. The general shape of the two figures is equivalent to Figs 2(a) and 2(b) respectively with two main differences: The curves are now flatter with more sharp changes, and the degradation temperature is shifted 200 degrees higher, i.e. 1800 K (1527°C). This is also illustrated in Fig. 4(b) where the rapid increase of CO, SiO, $CO_2$ and Si also occurs to a higher temperature, i.e. 1800 K (1527°C).

Once again it appears that titanium is entirely linked in its carbide form (Fig 4(a)) and that it has a negligible reactivity in the gas phase (Fig. 4(b)). The quantity of $TiC_x$ remains unchanged up to 1750 K (1477°C) and decreases above it as shown in Fig. 5. The same differences hold for the carbon content where now $TiC_x$ becomes understoichiometric at 1650 K (1377°C). However it has to be pointed out that, as in the conditions of Fig. 3, these variations are extremely weak and, even if they show evidence of the upper stability limit of the material in the corresponding conditions, they are not representative of a significant change in the composition and, consequently in the physical properties of the fibre.

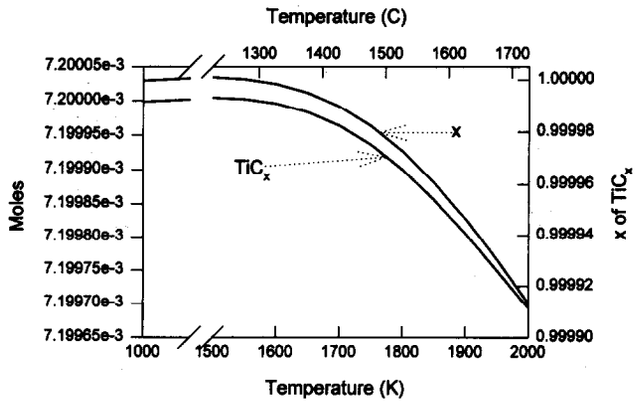


**Fig. 3.** Thermal evolution of one g-atom of Lox-M. Number of moles of $TiC_x$ (left) and carbon content of $TiC_x$ (right) in contact with one g-atom Ar as a function of treatment temperature.

## Experimental

The operating procedure and the main results of the thermogravimetric analysis (TGA) and of the SEM and the TEM characterization are reported

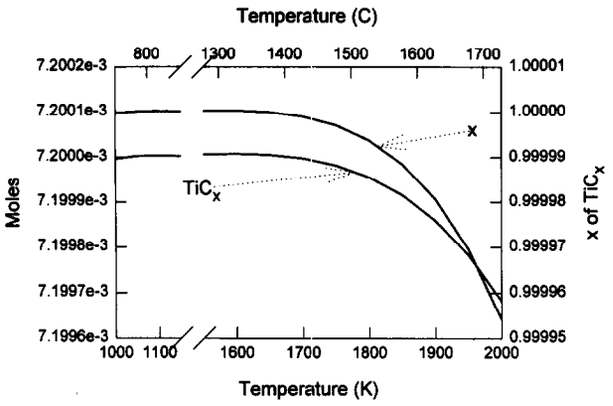


**Fig. 5.** Thermal evolution of one g-atom of Lox-M. Number of moles of $TiC_x$ (left) and carbon content of $TiC_x$ (right) in contact with $10^{-4}$ g-atom Ar as a function of treatment temperature.

in.[8] The operating conditions were chosen to be identical to the heat treatment conditions of the Nicalon® fibre, reported in Ref. 20.

In Fig. 6 the TG recordings for treatments at 1623, 1673 and 1773 K (1350, 1400 and 1500°C) are presented. In contrast to the 1573 K (1300°C) sample where the weight loss of the fibre had not reached a plateau at the end of the heat treatment, it appears that the duration of the treatment at each of the above temperatures was long enough to allow the material to reach a stable composition. This stabilization was produced after an almost equal weight loss for the three temperatures: 20·3, 18·3, and 21·8% respectively, to be compared to the reported weight loss of 25·6% for the NL-202 Nicalon® fibre at 2000 K (1727°C).[20]

The SEM characterization indicated that the shape and the dimensions of the 10 $\mu$m diameter fibres remain stable after the 1773 K (1500°C) treatment except for a slight increase of the surface roughness compared to the as-received material. However, TEM characterization revealed marked changes between these temperatures regarding the structure and the nanotexture of the fibre, as has been pointed out in Ref. 8 and will be next discussed.

The TEM investigation, showed that the as-received fibre has a nanometric porosity, and that it contains $\beta$-SiC nanocrystals and small free carbon units, both having a diameter less than 2 nm. Small stacks of 2–3 fringes of free carbon are shown in the $C_{002}$ Lattice Fringe (LF) image of Fig. 7 (arrows). They are made of basic structural units, (BSUs), i.e. the elemental entities common to many other carbonaceous materials, the diameter of which was determined to be less than 1 nm.[24] Silica was not detected at the extreme surface or within the fibre.

It was not possible to characterize the inner part of samples treated at 1623 K (1350°C) since, because of the high brittleness, ultramicrotomy did not yield any entire section. The 'in-place' particles, i.e. attached to the embedding resin, correspond to the external part of the filament. However, the

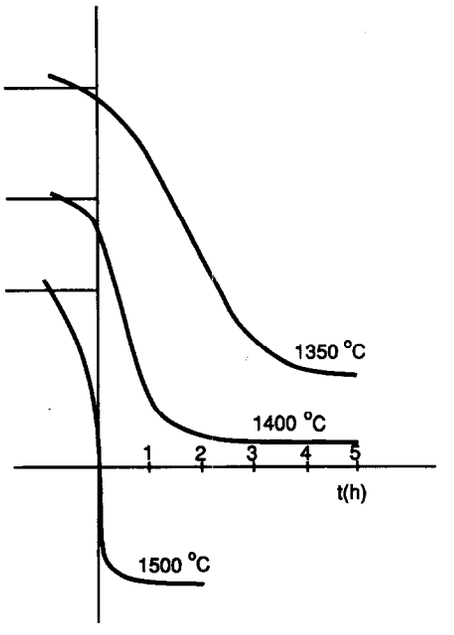


**Fig. 6.** TG analysis recordings for treatments of Lox-M at 1623, 1673, and 1773 K. From Ref. 8.

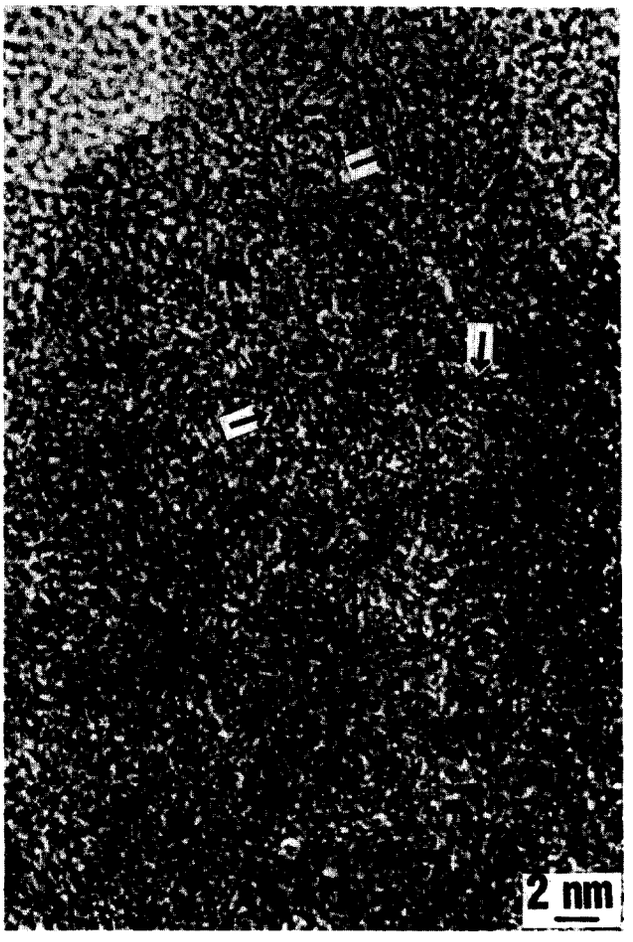


**Fig. 7.** $C_{002}$ LF image of as-received Lox-M. Arrows indicate BSU's. Similar to Fig. 3 in Ref. 8.

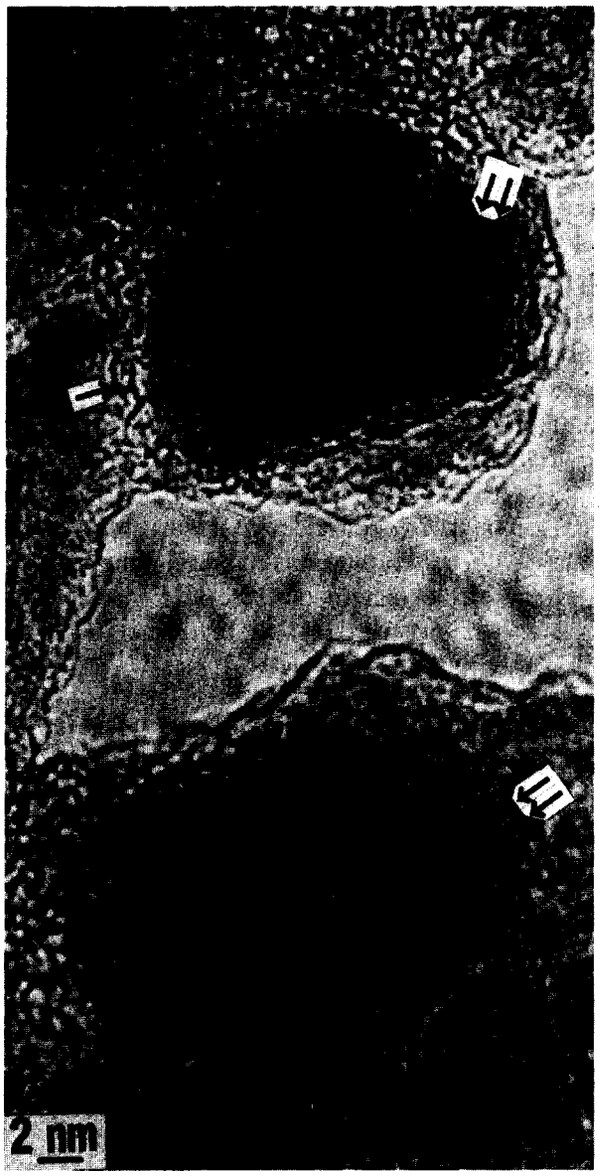


**Fig. 8.** $C_{002}$ and $SiC_{111}$ LF image of 1673 K heat treated Lox-M. Single arrow point a stack of degraded free carbon, one layer of which was partially consumed. This is a characteristic texture of activated polyaromatic carbon. Double arrows point $SiC_{111}$ lattice fringes. Similar to Fig. 5 in Ref. 8.

investigation of the 'out-of-place' particles provides a statistical idea of the features of the whole fibre. No significant differences were found between random particles and 'in-place' particles from the outer part of the fibre suggesting that the fibre is homogeneous. The major evolution between this and the as-received samples is that carbon is now better organized since BSUs have been associated both face-to-face and edge-to-edge forming stacks of 3–6 distorted layers. This association yields distorted fringes having an average length of ~3 nm. As was shown from 1673 K (1400°C) and 1773 K (1500°C) heat treated fibres, this organization takes place around each SiC crystal, in agreement with other SiC-based material.[20,25]

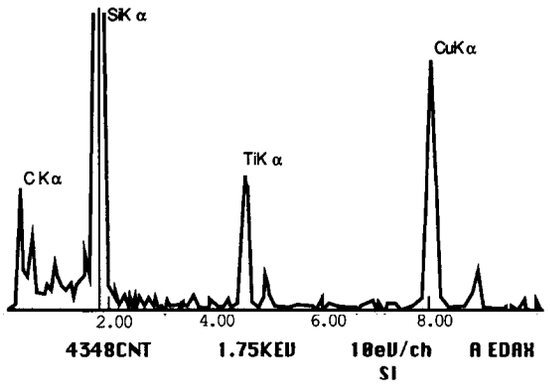


**Fig. 9.** EDS elemental analysis pattern for 1773 K treated Lox-M.

A $C_{002}$ and $SiC_{111}$ LF image of a 1673 K (1400°C) treated fibre is presented in Fig. 8.[8] At this temperature, SiC crystals have grown markedly up to 60 nm (to be compared to a maximum of 8 nm for the NL-202 fibre in identical conditions),[20] suggesting that the major degradation step has already occurred. Crystal growth is very fast as corresponding SAD patterns show polytypism marks, and free carbon seems degraded, although its aromatic layers remain oriented parallel to the crystalline faces. At 1773 K (1500°C) there is no marked evolution of the fibre except that SiC crystals become larger; their thickness is as high as 90 nm, again with a wide distribution in size.

It was not possible to evidence the titanium carbide either in Electron Diffraction pattern reflections, or in Dark Field (DF) TEM mode. While in the first case TiC reflections are too close to SiC for an unambiguous observation, in the second case TiC grains are not evidenced possibly because of their very small size or because titanium participates (at least in the original fibre) in the intergranular solid solution. The EDS elemental analysis, whose typical pattern is shown in Fig. 9 for a 1773 K (1500°C) treated fibre, did not reveal any significant difference in composition between the skin and the core of the fibre either at 1673 K (1400°C) or at 1773 K (1500°C).

## Discussion

The evolution in composition of the condensed species as a function of temperature, which is evidenced in Figs 2(a) and 4(a) illustrates the capacity of the fibre to support, without major alteration, the heat treatments in the selected experimental conditions. This is valid up to a temperature which is a function of the argon dilution and which is detected in the above diagrams by an abrupt change in composition, especially by the

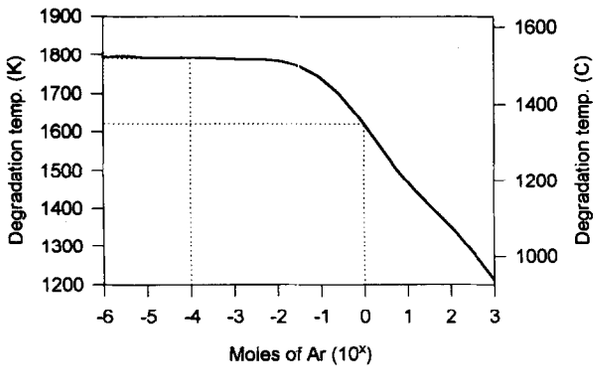


**Fig. 10.** Thermal evolution of Lox-M. Degradation temperature as a function of the number of moles of Ar available. Dotted lines correspond to the investigated conditions.

elimination of the free carbon, due to an endogenous oxidation mechanism leading to formation of SiC and CO. Following the results of the thermodynamic investigation, the Lox-M Tyranno® fibre is expected to change drastically in composition, morphology and hence physical properties in the range between 1600 and 1800 K (1327 and 1527°C).

The validity of these transition temperatures is studied in Fig. 10, where the degradation temperature is drawn as a function of the number of moles of Ar available in the calculations. As for the NL-202 Nicalon® fibre,[21] the degradation temperature does not depend on the dilution of the reactants up to approximately $10^{-2}$ g-atom Ar/g-atom. For higher dilution it decreases linearly with the logarithm of Ar quantity. From this figure it appears that, for a material containing no pores or cracks, only calculations made with $10^{-4}$ g-atom Ar/g-atom have a more general value and can represent the situation in the core, while calculations made with 1 g-atom Ar/g-atom qualitatively indicate that operating conditions are more severe at the external part, leading to lower values of the degradation temperature. It is worth noting that a similar behavior was evidenced by Luthra and Hee Dong[26] in carbon-fibre/oxide-matrix composites: The authors evaluated the chemical compatibility of different oxides with carbon at $T \approx 1873$ K (1600°C) and concluded that these materials are stable if they contain neither cracks nor pores allowing CO to escape.

The fact that the nanotextures of the as-received and of the 1623 K (1350°C) treated fibre are similar while at 1673 K (1400°C) degradation has already occurred, reveals the temperature interval within which degradation is initiated. In the same operating conditions NL-202 was found to be similar to the as-received material at 1523 K (1250°C), to present a skin-and-core effect at 1673 K (1400°C) and to be degraded at 1773 K (1500C).[20] No skin-and-core effect was observed during the degradation of the Lox-M. However, in view of the similarity between the two fibres concerning their precursors, their morphology and their properties, it is presumed that both present a diffusion-limited degradation mechanism. Additionally in the various ceramic materials such as Nicalon® 200 and other experimental Si–C–O and Si–C–N–O fibres investigated in the laboratory, brittleness during ultramicrotomy preparation is systematically important in the as received state and also remains elevated after low temperature treatments. This behaviour yields operating difficulties and often fragmentation. However, as soon as high temperature treatments have degraded the continuum, i.e. the cement between the SiC crystals, the diamond edge progresses among the nanometric crystals and fibres are cut considerably easier. For the investigated family of ceramic materials, this behaviour during ultramicrotomy may thus be considered as an indication of the existence of the interganular solid solution and also of the temperature domain where this solution is degraded. Lox-M behaves in a similar way: it is very brittle below 1623 K (1350°C) and much less above 1673 K (1400°C). Consequently, the degradation of the continuum and the corresponding skin-and-core effect in this fibre must occur between these two temperatures.

The thermodynamic simulation evidenced no difference between the chemical systems corresponding to Tyranno® and Nicalon® fibres. Indeed, Figs 2, 4 and 10 are identical to the corresponding figures for NL-202.[21] It can thus be deduced that degradation of the two fibres is initiated in the same temperature range. In that case, the relatively narrow temperature gap where the presumed skin-and-core effect takes place for Lox-M, compared with NL-202 (degradation of the Nicalon is initiated below 1673 K and is accomplished at 1773 K approximately), indicates that the progression of the skin-reactions to the core is faster in Tyranno®. A more rapid diffusion of the gaseous by-products may be responsible for this behavior due to a higher or more open porosity as is suggested by the lower density of Lox-M relative to NL-202: The two densities are 2·37 and 2·55 g $cm^{-3}$ respectively and only 6% of this difference is due to the difference in composition of the fibres.

Titanium does not seem to modify the chemical behavior of Lox-M relatively to NL-202 except that it combines with an equivalent quantity of carbon. The possible existence of stoichiometric titanium carbide in the original fibre or its formation during the heat treatment is in agreement with the Si–Ti–C phase diagram, whose 1473 K

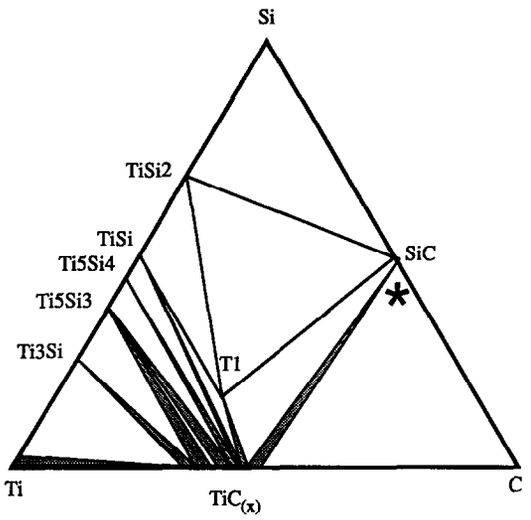


**Fig. 11.** Si–Ti–C phase diagram. Isothermal section at 1473 K, as calculated in Ref. 22. The initial composition of Lox-M is shown (★).

(1200°C) isothermal section is presented in Fig. 11.[22] As illustrated in this figure, the global composition point of the fibre is located at the interior of the SiC–TiC–C part of this diagram. Since this part of the isothermal section remains stable within a large temperature domain, it can be reasonably assumed that if titanium is not in solution in the original fibre, it will remain present in the form of stoichiometric TiC. The calculations showed that moderate quantities of oxygen are more likely to react with carbon and silicon rather than with titanium or titanium carbide. It is thus possible that in the investigated conditions, only a small shift of the location of the total composition of the fibre within the corresponding quaternary phase diagram takes place, relative to the Si–C–Ti ternary section. However, because of the departure of carbon from the fibre in the form of carbon monoxide but also because of the poor description of the $TiC_x$ phase leading to uncertainties concerning the shape of the phase diagram, a shift of the global composition above the degradation temperature at the exterior of the SiC–TiC–C triangle towards silicon carbide, i.e. a very low other-than-SiC compounds' composition, cannot be excluded.

The difference between the experimentally determined upper limit of 1673 K (1400°C), and the calculated value of 1800 K (1527°C) for the degradation of the fibre, can be attributed to the fact that the concept of a material composed of silicon carbide, carbon and silica, where the core is dissociated from the skin, is not enough powerful to describe and predict more precisely its thermal behavior. However, as was discussed in Ref. 21, the comparison between the thermochemical properties of silicon carbide fibers and of silicon oxycarbide black glass with $SiC+SiO_2+C$ mixed powder, as was investigated by multiple Knudsen cell mass spectrometry in Refs 27 and 28 respectively, showed that the measured pressures of SiO and CO gaseous species above the three materials were comparable. Therefore, the $SiC_xO_y$ solid solution can be replaced as a mixture of $SiC+SiO_2+C$ in the simulation, if the obtained results are considered exclusively in terms of the degradation temperature and of the gas phase composition above the fibre. The thermodynamic simulation is in this case helpful in order to illustrate, understand and predict the major reaction mechanisms responsible for the observed degradation. However, it has to be mentioned that other parameters may also be responsible for the observed difference between experimental results and thermodynamic predictions in similar operating conditions. One is related to the quality of the thermodynamic data adopted to describe the compounds participating in the chemical process. Although important research has already been performed on the chemical behavior of the Si–C–O[28] and of the Si–Ti–C[29] systems, more is needed to be done to improve their thermodynamic description. Other phenomena which have not been taken into account in the present work and which may also participate in the way the material is transformed during heat treatments are solid state diffusion and surface/interface kinetics. The quantification and modelization of their influence is a complex task, especially in the presence of poorly organized constituents.

## Conclusions

The evolution of the Lox-M Tyranno® fibre as a function of treatment temperature in inert gas atmosphere and atmospheric pressure was thermodynamically simulated by performing thermochemical calculations in the Si–C–O–Ti chemical system, and was compared to recently performed structural and nanotextural TEM investigations.

The environments in the core and at the skin of the fibre were differentiated in the calculations by considering different inert gas dilution of the reactants. The stability limit of the material was thus calculated to be at 1800 K (1527°C) or lower. At this temperature the available carbon is exhausted and the oxygen content is highly reduced. The main reaction products are silicon carbide and carbon and silicon monoxides. The stable configuration for titanium is expected to be stoichiometric titanium carbide which exhibits a pronounced stability in terms of quantity and stoichiometry

within a large temperature domain, in agreement with the Si–Ti–C phase diagram.

From the comparison of the results of the thermodynamic study and the TEM characterization of the Lox-M Tyranno® and of the NL-202 Nicalon® fibres it appears that the chemical behavior of the Si–C–O–Ti and of the Si–C–O systems is identical in the investigated conditions and that similar mechanisms govern the thermal degradation of the materials. However, the degradation process is completed faster in the case of Lox-M, possibly because of a more rapid diffusion of the gaseous reaction by-products through the core of the fibre.

## Acknowledgements

Thanks are due to Evelyne Fischer (THERMODATA) for help with the GEMINI2 software, to Pierre-Yves Chevalier (THERMODATA) for help with the thermodynamic data, to Jean-Paul Tricard (Elf-Aquitaine) for SEM facilities and to Takemi Yamamura (UBE Industries) for supplying the Tyranno® fibres.

## References

1. Yajima, S., Iwai, T., Yamamura, T., Okamura, K. & Hasegawa, Y., Synthesis of a polutitanocarbosilane and its conversion into inorganic compounds. *J. Mater. Sci.*, **16** (1981) 1349–55.
2. Murthy, V. S. R., Lewis, M. H., Smith, M. E. & Dupree, R., Structure and degradation of Tyranno fibers. *Materials Letters*, **8** (1989) 263–8.
3. Yamamura, T., Waku, Y., Ishikawa, T., Yamamoto, T., Shibuya, M., Suzuki, M., Nishi, T. & Nagasawa, T., In *Looking Ahead for Materials and Processes*, 8th SAMPE European Chapter, La Baule, France, 1987 pp. 19–28.
4. Hasegawa, Y., Fen C. X., Song, Y. C. & Tan, Z. L., Ceramic fibre from polymer precursor containing Si–O–Ti bonds. *J. Mater. Sci.*, **26** (1991) 3657–64.
5. Yamamura, T., Ishikawa, T., Shibuya, M., Hisayuki, T. & Okamura, K., Development of a new continuous Si–C–Ti–O fibre using an organometallic polymer precursor. *J. Mater. Sci.*, **23** (1988) 2589–94.
6. Yamamura, T., Development of high tensile strength Si–Ti–C fiber as an organometallic polymer precursor. *Am. Chem. Soc. Polymer. Preprints*, **25** (1984) 8–9.
7. Yamamura T. Shibuya, M., Ishikawa, T., Sato, M. & Hisayuki, T., Properties of a continuous Si–Ti–C–O fibers synthesized from an organometallic polymer. In *Japan–US Joint Seminar on Inorganic and Organometallic Polymers,* Nagoya, Japan, 1991.
8. Bourgerette, C., LeCoustumer, P., Monthioux, M. & Vahlas, C., TEM characterization of heat treated Tyranno fibers. In *Proceedings of the International Conference ECCM 6th High Temperature — Ceramic Matrix Composites*, eds R. Naslain, J Lamon & D. Doumeingts, 1993, pp. 67–74.
9. Scientific Group Thermodata Europe, available on line from THERMODATA, BP 66 F-38402 Saint Martin d'Hères, France and Royal Institute of Technology, S-10044, Stockholm, Sweden.
10. Barin, I., *Thermochemical Data of Pure Substances*. VCH, Weinheim, GER, 1989.
11. Gurvich, L. V., Veyts, I. V. & Alcock, C. B., *Thermodynamic Properties of Individual Substances*, 4th edition Vol 1 and 2. Hemisphere Publishing Corp., New York, 1990.
12. Sundman B. & Agren, J., A regular solution model for phases with several components and sublattices, suitable for computer applications. *J. Phys. Chem. Solids*, **42** (1981) 297–301.
13. Vahlas, C. Chevalier, P. Y. & Blanquet, E., Thermodynamic approach to the selective deposition of refractory metal silicides. *Calphad*, **13** (1989) 275–94.
14. Vincent, C., Dazord, J., Bouix, J. & Bernard, C., Calcul de l'energie libre de formation de Gibbs du carbure de titane $TiC_y$ par la methode des sous reseaux. Application a la determination de diagrammes de depot chimique en phase vapeur. *Thermochimica Acta*, **147** (1989) 1–15.
15. Pampouch, R., Ptak, W. S., Jonas, S. & Stoch, J., The nature of ternary Si–O–C phase(s) formed during oxidation of SiC. In *Proceedings of the 9th International Symposium on Reactivity of Solids*, eds. K. Direk, J. Habber & J. Novotny, 1980, pp. 674–84.
16. Yavouz, B. O. & Hench, L. L. Low temperature oxidation of SiC. *Ceram. Eng. Sci. Proc.*, **3** (1982) 596–600.
17. Lipowitz, J., Freeman, H. A., Chen, R. T. & Prack, E. R., Composition and structure of ceramic fibers prepared from polymer precursors. *Adv. Ceram. Mater.*, **2** (1987) 121–8.
18. Porte, L. & Sartre, A., Evidence for a silicon oxycarbide phase in the Nicalon silicon carbide fibre. *J. Mater. Sci.*, **24** (1989) 271–86.
19. Laffon, C., Flank, A. M., Lagarde, P., Laridgani, M., Hagege, R., Olry, P., Cotteret, J., Dixmier, J., Miquel, J. L., Hommel H. & Legrand, A. P., Study of Nicalon-based ceramic fibres and powders by EXAFS spectrometry, X-ray diffractometry and some additional methods. *J. Mater. Sci.*, **24** (1989) 1503–12.
20. LeCoustumer, P., Monthioux, M. & Oberlin, A., Understanding Nicalon® fiber. *J. Europ. Ceramic Soc.*, **11** (1993) 95–103.
21. Vahlas, C., Rocabois, P. & Bernard, C., Thermal degradation mechanisms of the Nicalon® fibre: A Thermodynamic Simulation. *J. Mater. Sci.*, in press.
22. Racault, C., Langlais, F. & Bernard, C., On the CVD of $Ti_3SiC_2$ from $TiCl_4$–$SiCl_4$–$CH_4$–$H_2$ gas mixtures. 1 — A thermodynamic approach. *J. Chemical Vapor Deposition* submitted for publication.
23. Dinsdale, A. T., SGTE Data for Pure Elements, NPL report DMA(A) 195, Sept. 1989.
24. Oberlin, A., High resolution TEM studies of carbonization and graphitization. In *Chemistry and Physics of Carbon*, Vol. 22, ed. P. A. Thrower, Marcel Dekker, NY and Bassel, 1989, pp. 1–143.
25. Monthioux, M., Oberlin, A. & Bouillon, E., Relationship between microstructure and electrical properties during heat treatment of SiC fibre precursor. *Comp. Sci. and Technol.*, **37** (1990) 21–37.
26. Luthra, K. L. & Hee Dong P., Chemical considerations in carbon-fiber/oxide-matrix composites. *J. Am. Ceram. Soc.*, **75**(7) (1992) 1889–98.
27. Rocabois, P., Chatillon, C. & Bernard, C., Mass spectrometry experimental investigation and thermodynamic calculation of the Si–C–O–(N) system and $Si_x$–$C_y$–$O_z$ fibre stability. In *Proceedings of the International Conference ECCM 6th. High Temperature — Ceramic Matrix Composites*, eds R. Naslain, J. Lamon & D. Doumeingts, 1993, pp. 93–100.
28. Rocabois, P., Chatillon, C. & Bernard, C., Multiple Knudsen cell mass spectrometric investigation of the evaporation of silicon oxicarbide glass. *Surface and Coatings Technology*, **61** (1993) 86–92.
29. Racault, C, Elaboration par voie solide et gazeuse et caractérisation physico-chimique de céramiques à base de $Ti_3SiC_2$, Thesis, Université de Bordeaux 1, France, 1993.